environmental microbiology
environmental microbiology reports

# 'Candidatus Adiutrix intracellularis', a homoacetogenic deltaproteobacterium colonizing the cytoplasm of termite gut flagellates (Trichonympha collaris)



| | |
|---|---|
| Journal: | *Environmental Microbiology and Environmental Microbiology Reports* |
| Manuscript ID: | EMI-2015-1306 |
| Manuscript Type: | EMI - Research article |
| Journal: | Environmental Microbiology |
| Date Submitted by the Author: | 09-Sep-2015 |
| Complete List of Authors: | Brune, Andreas; Max Planck Institute for Terrestrial Microbiology, Dept. of Biogeochemistry<br>Ikeda-Ohtsubo, Wakako; Tohoku University, Graduate School of Agricultural Science<br>Strassert, Jürgen; Max Planck Institute for Terrestrial Microbiology, Dept. of Biogeochemistry<br>Mikaelyan, Aram; Max Planck Institute for Terrestrial Microbiology, Dept. of Biogeochemistry<br>Tringe, Susannah; DOE Joint Genome Institute, |
| Keywords: | termite gut flagellates, intracellular symbionts, reductive acetogenesis, hydrogen, Deltaproteobacteria |
| | |

# '*Candidatus* Adiutrix intracellularis', a homoacetogenic deltaproteobacterium colonizing the cytoplasm of termite gut flagellates (*Trichonympha collaris*)

**Wakako Ikeda-Ohtsubo[1†], Jürgen F. H. Strassert[1,2], Tim Köhler[1], Aram Mikaelyan[1], Ivan Gregor[3,4], Alice C. McHardy[3,4], Susannah Green Tringe[5], Phil Hugenholtz[5,6], Renate Radek[2], and Andreas Brune[1]***

[1] *Department of Biogeochemistry, Max Planck Institute for Terrestrial Microbiology, Karl-von-Frisch-Strasse 10, 35043 Marburg, Germany*

[2] *Institute of Biology/Zoology, Free University of Berlin, Königin-Luise-Strasse 1–3, 14195 Berlin, Germany*

[3] *Computational Biology of Infection Research, Helmholtz Center for Infection Research, Inhoffenstraße 7, 38124 Braunschweig, Germany*

[4] *Department of Algorithmic Bioinformatics, Heinrich Heine University Düsseldorf, 40225 Düsseldorf, Germany*

[5] *Department of Energy Joint Genome Institute, Walnut Creek, California 94598, USA*

[6] *Australian Centre for Ecogenomics, The University of Queensland, Brisbane QLD 4072, Australia*

Running title: *A homoacetogenic deltaproteobacterium from termite guts*

*For correspondence. E-mail brune@mpi.marburg.mpg.de; Tel. (+49) 6421 178701

† Present address: Laboratory of Animal Products Chemistry, Graduate School of Agricultural Science, Tohoku University, Sendai 981-8555, Japan

## Summary

Termite gut flagellates are typically colonized by specific bacterial symbionts. Here we describe the phylogeny, ultrastructure, and subcellular location of '*Candidatus* Adiutrix intracellularis', an intracellular symbiont of *Trichonympha collaris* in the termite *Zootermopsis nevadensis*. It represents a novel, deep-branching lineage of uncultured *Deltaproteobacteria* widely distributed in intestinal tracts of termites and cockroaches. Fluorescence in situ hybridization and transmission electron microscopy revealed that the symbiont colonizes the cytoplasm of the flagellate near hydrogenosomes in the posterior part of the host cell and near the ectosymbiont '*Candidatus* Desulfovibrio trichonymphae' in the anterior part. The draft genome of '*Ca.* Adiutrix intracellularis' (~2 Mbp; > 91% complete) obtained from a metagenomic library allowed us to assess its metabolic potential. The presence of a complete gene set encoding the Wood-Ljungdahl pathway, including a hydrogen-dependent carbon dioxide reductase (HDCR), substantiates previous claims that the symbiont is capable of reductive acetogenesis from $CO_2$ and $H_2$. The HDCR genes are most closely related to homologs from homoacetogenic spirochetes and firmicutes, suggesting that the deltaproteobacterium acquired the capacity for homoacetogenesis via lateral gene transfer. The presence of genes for an alternative nitrogenase (AnfHDK) and the biosynthesis of essential amino acids and co-factors indicate the nutritional nature of the symbiosis.


Keywords: *termite gut flagellates, intracellular symbionts, reductive acetogenesis, hydrogen, Deltaproteobacteria*

## Introduction

Flagellate protists are abundant and characteristic members of the gut microbiota in lower termites (Brune and Ohkuma, 2011; Brune 2014). Originally described as "parasites" (Leidy, 1881), their essential role in the symbiotic digestion of lignocellulose was established already during the first half of the 20th century (Cleveland, 1925; Hungate 1943). Flagellates of the genus *Trichonympha* (class Parabasalia) are found in members of several termite families, and their diversity has been described in numerous morphological and molecular studies (see Kirby, 1932; Brugerolle and Radek, 2006; Carpenter et al., 2009; Ohkuma et al., 2009).

Most termite gut flagellates are colonized by specific bacterial symbionts, often in multiple associations (Hongoh and Ohkuma, 2011; Ohkuma and Brune, 2011). Some of them represent deep-branching lineages that were most likely acquired by ancestral flagellates at an early stage of their evolutionary radiation. In the genus *Trichonympha*, examples are '*Candidatus* Endomicrobium trichonymphae' (Stingl et al., 2005), which belongs to a termite-specific clade in the Elusimicrobia phylum and occurs exclusively in flagellates of *Trichonympha* Cluster I (Ohkuma et al., 2007; Ikeda-Ohtsubo and Brune, 2009), and '*Candidatus* Ancillula trichonymphae', a lineage in a termite-specific clade of *Actinobacteria* that occurs in flagellates of *Trichonympha* cluster II (Strassert et al., 2012).

While such "primary" symbionts seem to have cospeciated with their respective hosts over a longer evolutionary time frame (Noda et al., 2007; Ikeda-Ohtsubo and Brune, 2009; Desai et al., 2010), there are many examples of "secondary" symbionts that were independently acquired by individual host species, most likely long after the symbiosis with the primary symbiont had been established (Ohkuma and Brune, 2011). A prominent example of such recent associations is '*Candidatus* Desulfovibrio trichonymphae', which colonizes either the cytoplasm (in *Reticulitermes speratus*) or cell surface (in *Incisitermes marginipennis*) of *Trichonympha* species (Sato et al., 2009; Strassert et al., 2012) and belongs to a lineage within the *Desulfovibrio* complex that is commonly encountered also in the intestinal tracts of flagellate-free termites and other insects.

However, diversity studies of termite gut microbiota have identified also a second, much more deep-branching clade of *Deltaproteobacteria*, the 'Rs-K70 group' (e.g., Hongoh et al., 2003; 2005; Shinzato et al, 2007; Warnecke et al., 2007), which was abundantly represented in clone libraries of bacterial 16S rRNA genes obtained from capillary-picked *Trichonympha*

suspensions of the dampwood termite *Zootermopsis nevadensis* (JQ993543; Ikeda-Ohtsubo 2007, Strassert et al., 2012). Rosenthal et al. (2013) localized transcripts of a hydrogenase-linked formate dehydrogenase gene (*fdh*$F_{Sec}$) to single cells of an almost identical phylotype (JX974519) of uncultured *Deltaproteobacteria* from the gut of this termite and documented its association with *Trichonympha* flagellates. The observations that the homolog assigned to the symbiont was the most highly expressed *fdh*$F_{Sec}$ gene in the gut implicated this flagellate symbiont – and possibly also other members of the Rs-K70 group – as major players in reductive acetogenesis from $H_2$ and $CO_2$ in termite guts (Rosenthal et al., 2013).

Here we provide a detailed phylogenetic, ultrastructural, and metabolic characterization of an endosymbiont '*Candidatus* Adiutrix intracellularis', from this Rs-K70 group. We analyzed its relationship to other members of the Rs-K70 group from the intestinal tracts of insects and determined its host specificity and subcellular location by fluorescence in situ hybridization (FISH) and transmission electron microscopy (TEM). In addition, we reconstructed the metabolism of the endosymbiont from its draft genome, which was assembled from a metagenomic library prepared from genomic DNA of the microbial symbionts associated with the *Trichonympha* flagellates of *Z. nevadensis*.

## Results and discussion

### *Phylogeny*

The 16S rRNA gene sequences of '*Ca.* Adiutrix intracellularis' previously obtained from capillary-picked *Trichonympha* suspensions consisted of several, almost identical phylotypes (99.4–99.9% sequence similarity) that clustered among other representatives of the Rs-K70 group recovered from the intestinal tracts of termites (Fig. 1). With a specific primer pair designed on the basis of these sequences, we obtained additional clones from hindgut DNA of several cockroaches (*Blaberus giganteus*, *Gromphadorrhina portentosa*, and *Nauphoeta cinerea*), lower termites (*Zootermopsis nevadensis, Cryptotermes secundus*), and a cetoniid beetle larva (*Pachnoda ephippiata*). Together with several clones recently obtained from other termites and cockroaches (Mikaelyan et al., 2015), they all clustered according to their respective host groups (Fig. S1). Interestingly, the clones from *Z. nevadensis* comprised additional, previously unknown phylotypes that were distinct from '*Ca.* Adiutrix

intracellularis' and may represent symbionts of other flagellate species or free-living members of the Rs-K70 group.

The next relatives of the clones in the Rs-K70 group are uncultured bacteria from terrestrial and marine environments (Fig. 1). '*Ca.* Adiutrix intracellularis' shares only very low sequence similarity (86.1–86.6%) with the 16S rRNA genes of its closest cultured relatives, namely *Desulfatiglans* (*Desulfobacterium*) *anilini*, *Desulfoarculus baarsii*, and *Desulfomonile tiedjei*, which are each considered to represent a different order of *Deltaproteobacteria* (Kuever, 2014), underlining the deep-branching nature of the novel lineage.

***Localization***

FISH analysis of *Trichonympha* suspensions from *Z. nevadensis* with a newly designed oligonucleotide probe revealed that '*Ca.* Adiutrix intracellularis' exclusively colonized flagellates with the morphology of *Trichonympha collaris* (Fig. 2). Host specificity was confirmed by simultaneous hybridization with a probe specific for this flagellate species (Fig. S2A–D). Cells of '*Ca.* Adiutrix intracellularis' were distributed throughout the cytoplasm of the host cell, but showed highest densities in the anterior region, which is characterized by the brighter, concentrated signal on the collar (Fig. 2A, C; Fig. S2B, D). The location of '*Ca.* Adiutrix intracellularis' differs from that of '*Ca.* Endomicrobium trichonymphae', which preferentially colonizes the posterior part of the cell (Ikeda-Ohtsubo and Brune, 2009; Fig. S2E, F).

Flagellates of the genus *Trichonympha* are often colonized by '*Ca.* Desulfovibrio trichonymphae', which forms a monophyletic lineage of uncultivated *Deltaproteobacteria* in termite guts. Originally identified as endosymbionts of *Trichonympha agilis* in *Reticulitermes speratus* (Sato et al., 2008), a member of this lineage has also been detected in capillary-picked *Trichonympha* suspensions of *Z. nevadensis* (Strassert et al., 2012). Simultaneous hybridization of *T. collaris* with FISH probes specific for '*Ca.* Adiutrix intracellularis' and '*Ca.* Desulfovibrio trichonymphae' confirmed that the former are found throughout the host cell, whereas the latter are restricted to the anterior part, oriented in rows parallel to the surface grooves (Fig. 2D).

***Ultrastructure***

TEM of ultrathin sections of *Trichonympha* cells from *Z. nevadensis* confirmed the simultaneous presence of bacterial cell types with distinct morphologies in the anterior region.

One morphotype consists of short, irregular rods of variable diameter (0.5–0.6 µm) and length (0.8–1.9 µm; $n = 25$). The cells have slightly pointed ends and a somewhat irregular appearance. The wide electron-lucent space surrounding the cytoplasmic membrane has a highly contrasted outermost border, which resembles an outer membrane of the symbiont more than a vacuolar membrane of the host (Fig. 3A). The cells are characterized by electron-dense glycogen-like granules in their cytoplasm and were observed both in the anterior and posterior part of the host cell. In the posterior region, they were often situated close to hydrogenosomes (Fig. 3A). In the anterior part, they colonized the cytoplasmic protrusions between the multiple rows of flagella (Fig. 3B), the rostral tube, and the anterior cell pole (Fig. S3). Their morphology, subcellular arrangement and intracellular distribution were consistent with those of '*Ca.* Adiutrix intracellularis' in the FISH analyses (Fig. 2, Fig. S3).

The other morphotype is also rod-shaped, but much smaller (0.2–0.3 µm diameter, 1.1–1.9 µm length; $n = 13$), with a regular circumference and rounded ends (Fig. 3B). The cells are located on the surface of the cytoplasmic lamellae, often in proximity to cells of the first morphotype (Fig. 3B, C), and are laterally attached in deep pockets of the cytoplasmic membrane of the host. Occasionally, cells of the second morphotype were observed also within the cytoplasm of *Trichonympha* flagellates (not shown). These features are consistent with the morphology and distribution of '*Ca.* Desulfovibrio trichonymphae' in the FISH analyses (Fig. 2D). The regular arrangement of the cells along the cytoplasmic lamellae of the host cell (Fig. 3B) closely resembles the situation of the *Desulfovibrio* ectosymbionts of *Trichonympha globulosa* in *Incisitermes marginipennis* (Strassert et al. 2012).

The results of our current study provided an opportunity to revisit the exquisite work of Harold Kirby (1932), who has provided a detailed morphological description of the *Trichonympha* species in *Zootermopsis* termites on the basis of light microscopy. His observation of multiplying "peripheral granules" in the anterior end of *T. collaris* (collar and following surface ridges; Fig. S3) and his description of the rostrum having "the appearance of a collar striped with granular bands" bear a striking resemblance to the FISH micrographs of the dual hybridization of '*Ca.* Adiutrix intracellularis' and '*Ca.* Desulfovibrio trichonymphae' (Fig. 2D).

***Genome sequence***

A 16S rRNA gene library prepared from genomic DNA of the microbial symbionts associated with a suspension of *Trichonympha* flagellates from *Z. nevadensis* yielded 353 bacterial clones. The majority of the clones (50%) represented '*Endomicrobium trichonymphae*', the primary endosymbiont of these flagellates (Ikeda-Ohtsubo, 2007; Strassert et al., 2012). The second largest group (21%) was '*Ca.* Adiutrix intracellularis', followed by '*Ca.* Desulfovibrio trichonymphae' (17%) and other, much less abundant groups (for details, see Table S1). The majority of the 73 clones assigned to '*Ca.* Adiutrix intracellularis' represented the phylotype Adiu1 (AB972401), which is identical to that recovered in our previous studies (JQ993543; Ikeda-Ohtsubo 2007, Strassert et al., 2012).

The draft genome of strain Adiu1 (IMG Genome ID: 2556793040) was obtained through shotgun sequencing of this DNA, followed by sequence assembly and a combination of automated and manual binning. The sequence bin of strain Adiu1 consists of 155 scaffolds (2,076,491 bp) and has an N50 value of 23,926, which is much higher than that of any other bin in the dataset (Table S1). The draft genome contains one set of rRNA genes, 48 tRNA genes for all amino acids, and a near complete set (> 91%) of single-copy genes present in most bacterial genomes, including the most-closely related *Deltaproteobacteria* (Garcia Martin et al., 2006; Table S2).

The estimated genome size of strain Adiu1 is much smaller (ca. 2.3 Mb) and its coding density (60.1%) is much lower than the genome size and coding density in its closest relatives, *Dg. anilini* (4.67 Mb, 85.2%) and *Da. baarsii* (3.66 Mb, 91.1%), which indicated genome erosion in the endosymbiont. Also the G+C content of the genome is considerably lower in strain Adiu1 (43.3 mol%) than in its relatives (58.8 and 65.7 mol%, respectively). Almost the half (46.2%) of the 1,520 protein-coding genes in the Adiu1 genome gave highest BLAST scores against the genomes of other *Deltaproteobacteria* (Table S3). Of these genes, the majority had best matches against *Desulfobacterales* (27%), *Desulfovibrionales* (25%), and *Syntrophobacterales* (16%); the rest was either unassigned (22%) or showed an affinity to other phylogenetic groups (e.g., *Firmicutes*, 11%; *Gammaproteobacteria*, 3.5%). Such apparent heterogeneity in the phylogenetic origin of the coding genes is present also in *Da. baarsii* and *Dg. anilini*, which is not entirely unexpected considering that each of these strains represents a separate, deep-branching lineage of *Deltaproteobacteria* that is only poorly represented among sequenced genomes (Table S3; Suzuki et al., 2014).

***Wood-Ljungdahl pathway***

Although the closest relatives of '*Ca.* Adiutrix intracellularis' are sulfate-reducing *Deltaproteobacteria*, the draft genome of strain Adiu1 lacks the genes for key enzymes of sulfate reduction (Table S4). This includes *dsrAB* encoding alpha and beta subunits of dissimilatory sulfite reductase, *aprAB* for adenosine-5'-phosphosulfate reductase (APS reductase), *sat* for sulfate adenylyltransferase (ATP sulfurylase), and *sulP* for a sulfate permease (SulP). Also genes for cytochrome synthesis (i.e., the heme-specific branch of the tetrapyrrole biosynthesis pathway) and other important elements involved in sulfate reduction (e.g., Qmo and DsrMKJOP) were not found.

Instead, the genome contains the complete set of genes required for the Wood–Ljungdahl pathway of reductive acetogenesis (Table S4 and S5; Schuchmann and Müller, 2014). They include homologs of *fhs* for formyltetrahydrofolate synthetase (FTHFS), *folD* for bifunctional formyltetrahydrofolate cyclohydrolase/methylenetetrahydrofolate dehydrogenase (FolD), *ftcD* for formimidoyltetrahydrofolate cyclodeaminase (FTCD), *metF* and *metV* for large and small subunits of 5,10-methylenetetrahydrofolate reductase (MetFV), and *acsABCDE* for the subunits of the bifunctional carbon monoxide dehydrogenase/acetyl-CoA synthase (CODH/ACS) (Fig. 4; Table S5). The absence of the acetyl-CoA synthetase (*acs*) of acetate-oxidizing sulfate reducers and the presence of phosphotransacetylase (*pta*) and acetate kinase (*ack*), which are commonly used for energy conservation in acetate-producing sulfate reducers and homoacetogenic bacteria (Table S4, S5), indicate that the pathway operates in the reductive direction.

The strongest argument for a reductive acetyl-CoA pathway in '*Ca.* Adiutrix intracellularis', however, is the presence of gene sets coding for two hydrogen-dependent $CO_2$ reductases (HDCR, Fig. 4; Fig. 5), the key enzyme for the hydrogenation of $CO_2$ to formate in the homoacetogenic bacterium *Acetobacterium woodii* (Schuchmann and Müller, 2014). Like other homoacetogens, such as *Treponema primitia* (Matson et al., 2010) and *A. woodii* (Poehlein et al., 2013), the genome of strain Adiu1 contains two separate gene clusters of HDCR components, which include the genes for a selenium-free and a selenium-containing variant of a putative formate dehydrogenase H (*fdhF1* and *fdhF2*), a gene encoding the large subunit of an [FeFe] hydrogenase (*hydA2*), and three genes (*hycB1/2/3*) for the small electron transfer subunits of the complex, each following one of the genes for the large subunits. The

208 *fdhF2* homolog contains the in-frame stop codon TGA involved in the incorporation of
209 selenocysteine (Sec) into proteins (Zinoni et al., 1987).

210 The capacity for homoacetogenesis is unusual among *Deltaproteobacteria* and has been
211 demonstrated so far only for the sulfate-reducing *D. phosphitoxidans* grown in the absence of
212 sulfate (Schink et al., 2002). Most of the genes for the Wood-Ljungdahl pathway in the
213 genome of strain Adiu1 are most similar to those in the most closely related sulfate-reducing
214 *Deltaproteobacteria* (Fig. 4), which either oxidize acetate to $CO_2$ (*Dg. anilini* and *Da. baarsii*;
215 Schnell et al., 1989; Widdel and Bak, 1992) or are homoacetogenic (*D. phosphitoxidans*;
216 Schink et al., 2002). By contrast, the homologs of the entire HDCR modules show the highest
217 similarities to those of homoacetogenic *Spirochaetes* and *Firmicutes* (Fig. 4; Table S5). This
218 suggests that '*Ca.* Adiutrix intracellularis' acquired the capacity for homoacetogenesis by
219 lateral gene transfer.

220 ***Energy conservation***

221 Homoacetogens maximize the production of reduced ferredoxin using [FeFe] hydrogenases
222 that couple the endergonic reduction of ferredoxin with the exergonic reduction of $NAD^+$
223 (electron bifurcation; see Schuchmann and Müller, 2014). The genome of strain Adiu1
224 possesses two gene cassettes (*hydABC* and *hndABC*; Table S5), which encode homologs of
225 soluble, electron-bifurcating [FeFe] hydrogenases in *Moorella thermoacetica* (HydABC;
226 Wang et al., 2013) and *A. woodii* (HydABCD; Schuchmann and Müller, 2012) that catalyze
227 the concomitant reduction of ferredoxin and $NAD^+$ with 2 $H_2$, and an $NADP^+$-dependent
228 [FeFe] hydrogenase from *Desulfovibrio fructosovorans* (HndABCD; Malki et al., 1995),
229 respectively. Both gene sets show highest sequence similarities to their homologs in
230 homoacetogenic firmicutes (*Sporomusa ovata*, *Acetonema longum*), and in the case of
231 *hndABC*, also the homoacetogenic *T. primitia* (Table S5).

232 The energetic coupling of the Wood-Ljungdahl pathway to energy conservation in the
233 homoacetogens investigated to date involves either a membrane-bound Rnf complex
234 (homoacetogens without cytochromes; e.g., *A. woodii*) or an energy-converting hydrogenase
235 (Ech) complex (homoacetogens with cytochromes; e.g., *M. thermoacetica*). In both cases, the
236 free energy change during the oxidation of reduced ferredoxin with a more positive electron
237 acceptor ($NAD^+$ or $H^+$) is used to generate a sodium- or proton-motive force across the
238 cytoplasmic membrane (Schuchmann and Müller, 2014).

However, there is no evidence for the presence of an Rnf complex or an Ech-like [NiFe] hydrogenase in the draft genome of strain Adiu1. The only candidate for an electrogenic proton or sodium pump is encoded by a gene cluster coding for the 11 core subunits of complex I (*nuoABCDHIJKLMN*), the common elements of the membrane-bound NADH-ubiquinone oxidoreductase complex (Nuo), and the $F_{420}$-methanophenazine oxidoreductase complex (Fpo). This complex has most likely evolved from [NiFe] hydrogenases that lost their [NiFe] cluster and gained new functions by acquiring additional electron-transferring subunits, e.g., NuoEFG or FpoFO (Moparthi and Hägerhäll, 2011). Although the gene sets coding for 11-subunit complexes are present in the genomes of many bacteria and archaea, their interacting partner proteins or the redox process catalyzed by the respective complex are often unclear (Moparthi and Hägerhäll, 2011).

Notably, the genes that encode methylene-THF reductase (*metVF*) in '*Ca.* Adiutrix intracellularis' are preceded by genes that encode homologues of a small protein (*mvhD*) and a soluble electron-bifurcating heterodisulfide reductase (*hdrA*); while the *hdrBC* genes are on a different contig (Fig. S4). The *hdrCBA-mvhD-metVF* gene cluster from the homoacetogenic *M. thermoacetica* encodes a heterohexameric complex of MetFV, HdrABC and MvhD that reduces methylene-THF or oxidizes NADH with benzylviologen as artificial electron donor/acceptor, which led to the proposal that the complex is an electron-bifurcating enzyme that depends on a second, so far unidentified electron donor/acceptor (Mock et al., 2014).

Inspired by the ferredoxin-oxidizing activity of the Fpo-like 11-subunit complex in *Methanosaeta thermophila* (Welte and Deppenmeier, 2014) and its potential interaction with heterodisulfide reductase (HdrD) in *Methanomassiliicoccales* (Lang et al., 2015), we propose that the 11-subunit complex of '*Ca.* Adiutrix intracellularis' oxidizes ferredoxin and transfers the reducing equivalents to the cytoplasmic HdrCBA/MvhD/MetVF complex that reduces methylene tetrahydrofolate and $NAD^+$ in an electron-bifurcating reaction (Fig. 4). It is worth noting that the same gene cluster is present also in other homoacetogens that lack Rnf and in sulfate reducers that oxidize acetate via the Wood-Ljungdahl pathway (Table S5).

### *Carbon metabolism*

The draft genome of '*Ca.* Adiutrix intracellularis' contains a complete set of genes necessary for the Embden-Meyerhof pathway (EMP) (Table S5). Uptake and phosphorylation of hexoses proceeds via a phosphotransferase system (PTS), which consists of single gene sets

for the general cytoplasmic components (*ptsIH* for Enzyme I and HPr) and the sugar-specific Enzyme II complex (*manXYZW*), which has the same four-subunit structure (i.e., separate *manX* and *manW* genes for the IIA and IIB domains as the mannose/glucose permease of *Vibrio furnissii*; Bouma and Roseman, 1996). The presence of genes encoding glucose-6-phosphate isomerase (*pgi*) and phosphomannose isomerase (*manA*) indicates that the hexose 6-phosphates produced by the PTS are shuttled into the EMP pathway via fructose 6-phosphate (Fig. 5), but since PTS systems typically transport a number of different sugars, the exact nature of the substrate(s) provided by the host remains unclear.

The presence of all genes required for gluconeogenesis and for the biosynthesis and degradation of glycogen is in agreement with the assumption that the electron-dense inclusions in the cytoplasm of '*Ca.* Adiutrix intracellularis' are glycogen granules (Fig. 3). The presence of genes encoding a $Na^+$/alanine symporter and an alanine dehydrogenase suggests that alanine can be utilized as carbon and nitrogen source.

A pyruvate:ferredoxin oxidoreductase (PFOR) encoded by *porABDG* connects glycolysis/gluconeogenesis with the Wood-Ljungdahl pathway and intermediary metabolism (Fig. 5). Pyruvate carboxylase (encoded by *pyc*), malate dehydrogenase (oxaloacetate-decarboxylating, *maeA*), fumarate hydratase (*fumAB*), aspartate ammonia-lyase (*aspA*) and L-aspartate aminotransferase (*aspB*) mediate between the reductive branch of the TCA cycle and nitrogen metabolism (Fig. 5). Citrate is most likely produced by a *Re*-citrate synthase encoded by one of the gene homologs of isopropylmalate/homocitrate/citramalate synthase, as in the case of *Syntrophus aciditrophicus* (Kim et al., 2013). The oxidative branch of the TCA cycle is incomplete; as in many anaerobic bacteria, the genes for 2-oxoglutarate dehydrogenase and succinate dehydrogenase are absent (Fig. 5).

***Nitrogen fixation and ammonia assimilation***

The draft genome of Adiu1 contains a gene cluster encoding an (alternative) Fe-nitrogenase (Anf) complex (Fig. S5). It comprises the genes for the structural proteins (*anfHDK* and *anfG*), an iron-containing accessory protein (*anfO*), and an activator required for their transcription (Fig. S5). It is located on the same 13.7 kb-scaffold as two genes (*glnK1* and *glnK2*) encoding regulatory proteins and is similar in structure to the *nifHDK* cluster of many nitrogen-fixing bacteria (Fig. S5). Homologs of genes involved in the assembly of nitrogenase components and the incorporation of iron into the active center (*nifB*, *nifS*, and *nifU*) are also

present (Table S5). The genome contains homologs a glutamine synthetase (*glnA*) and glutamate synthase (*gltBD*) for the assimilation of ammonia. The location of *glnB* homologs (*glnK1* and *glnK2*) encoding for the regulatory protein P-II directly downstream of the gene for the ammonia transport protein (*amt*) indicates that nitrogen metabolism in '*Ca.* Adiutrix intracellularis' is regulated the same way as in *Escherichia coli* (Javelle et al., 2004). The iron-only cofactor (FeFeco) required by the Anf-type nitrogenase is most likely synthesized by a pathway related to the biosynthesis of the molybdenum-containing cofactor (FeMoco) (Yang et al., 2014), as indicated by the presence of the corresponding genes in the draft genome (Table S5).

Phylogenetic analysis revealed that the *anfH* gene of '*Ca.* Adiutrix intracellularis' belongs to a termite-specific cluster of *nifH* genes that belongs to Group II nitrogenases and comprises homologs of termite gut bacteria from different phyla (Fig. S6). It includes the flagellate symbiont '*Ca.* Armantifilum devescovinae', one of several lineages of nitrogen-fixing *Bacteroidales* (Arma Cluster II) that colonize cytoplasm and surface of termite gut flagellates and cospeciate with their respective hosts (e.g., Hongoh et al., 2008a; Desai and Brune, 2012). Since the primary and secondary symbionts (*Ca.* Endomicrobium and *Ca.* Desulfovibrio) of *Trichonympha agilis* lack the capacity for $N_2$ fixation (Hongoh et al., 2008b; Sato et al., 2009), the acquisition of a third symbiont by *T. collaris* may serve to complement this missing function.

***Amino acid and cofactor biosynthesis***

The draft genome of Adiu1 contains almost complete gene sets for the biosynthesis of all standard amino acids except asparagine (Fig. S7). The absence of asparagine synthetase suggests that asparagine must be acquired from the environment, most likely via the ATP-binding cassette (ABC) transporter of polar amino acids encoded by the *gln* gene cluster (Table S5). The presence of the genes for lysine biosynthesis via the meso-diaminopimelate pathway is in agreement with the assumption that the homolog of isopropylmalate/homocitrate/citramalate synthase is not involved in amino acid biosynthesis but encodes a citrate synthase (Table S4, also see Carbon metabolism). In addition, the draft genome contains all genes required for the biosynthesis of selenocysteine, which is an essential component of the catalytic center of $FDH_H$-Sec in the HDCR enzyme complex (see Wood-Ljungdahl pathway). Like all other genes coding for components of this complex, also

*selA* and *selD* (encoding seryl-tRNA selenium transferase and selenide, water dikinase) are most closely related to their homologs in *Firmicutes* (Table S5).

Coenzyme $B_{12}$ is essential for both the methyl and carboxyl branches of the Wood-Ljungdahl pathway. The draft genome of Adiu1 contains an almost complete set of genes required for the biosynthesis of cobalamin via precorrin-2 (Table S4). '*Ca.* Adiutrix intracellularis' lacks the *cbiJ* gene encoding an analog of precorrin-6x reductase (CobK), as in other *Deltaproteobacteria* and a number of archaea (Rodionov et al., 2004), suggesting it is probably not necessary for the biosynthesis of cobalamin. The presence of a vitamin $B_{12}$ transporter (encoded by *btuBCD*; Table S5) may allow '*Ca.* Adiutrix intracellularis' to provide vitamin $B_{12}$ to its host.

The draft genome of Adiu1 contains all genes required for the biosynthesis of riboflavin, NAD, siroheme, and menaquinone (Table S5). Although the genes for the biosynthesis of coenzyme A from pantothenate are present, the pathway leading to this precursor seems to be absent. Also the genes involved in the biosynthesis of biotin and tetrahydrofolate (THF) are absent or incomplete, respectively, suggesting that the endosymbiont depends on the external supply of these compounds. A requirement for THF precursors in a homoacetogen is not unprecedented; also *T. primitia* depends on the cross-feeding of 5'-formyl-THF by other gut bacteria in the termite guts (Graber and Breznak, 2005).

***Ecology and evolution***

Reductive acetogenesis from $H_2$ and $CO_2$ is the major hydrogen sink in the hindgut of wood-feeding termites, and there is a large body of evidence for a major role of spirochetes in this process, which typically form a large proportion of the bacterial microbiota of wood-feeding species (see reviews by Breznak, 2000; Breznak and Leadbetter, 2006; Brune, 2014). After the isolation of *T. primitia*, the first representative of the phylum Spirochaetes that was capable of reductive acetogenesis (Leadbetter et al.,1999; Graber and Breznak, 2004), numerous studies have documented the importance of related lineages from the *Treponema* I clade in termite guts based on diversity and expression profiles of phylogenetic and functional marker genes or on metagenomic approaches (e.g., Ottesen et al., 2006; Pester and Brune 2006; Warnecke et al., 2007; Zhang et al., 2011).

Therefore, it was quite surprising when Rosenthal et al. (2013) reported that spirochetes may not be the only organisms that contribute importantly to reductive acetogenesis is termite guts.

Using microfluidic multiplex digital PCR, they showed that the two most abundant *fdhF* gene transcripts in the gut of *Zootermopsis nevadensis* belong to an uncultured deltaproteobacterium (phylotype ZnDP-F1, JX974519) with 99.9% sequence similarity to the 16S rRNA gene of '*Ca.* Adiutrix intracellularis', and documented that cells of this phylotype are associated with *Trichonympha* flagellates (Rosenthal et al., 2013). The sequences of clones ZnHcys (GQ922420) and ZnD2sec (GU563467) encode a cysteine-dependent and selenocysteine-dependent variant of formate dehydrogenase H (a component of HDCR) and are almost identical (99%) to the nucleotide sequences of *fdhF1* and *fdhF2* in the Adiu1 genome. Although the authors reported that the cells of ZnDP-F1 phylotype were associated with the surface of the protist, their images would be also consistent with an intracellular location. Therefore, it seems safe to conclude that the deltaproteobacterial symbiont of *Trichonympha* flagellates reported by Rosenthal et al. (2013) is identical to '*Ca.* Adiutrix intracellularis'.

Reductive acetogenesis is quite unusual for *Deltaproteobacteria*, but our genome analysis of '*Ca.* Adiutrix intracellularis' corroborates these exciting findings by documenting the presence of the full set of genes required for reductive homoacetogenesis. In addition, it sheds light on the evolutionary origin of the homoacetogenic capacity in this novel lineage of *Deltaproteobacteria*, which apparently complemented an existing Wood-Ljungdahl pathway by acquiring a few key genes encoding HDCR from other bacterial lineages, most likely by lateral gene transfer. It is an intriguing question whether this metabolic change happened in an ancestral member of the Rs-K70 cluster, which would imply that the entire order-level cluster is homoacetogenic. However, it is also possible that the putatively free-living relatives of '*Ca.* Adiutrix intracellularis' present in other insects are still sulfate reducers, and the gene transfer rendering them homoacetogenic was a more recent event – and possibly a prerequisite for colonization of the intracellular habitat. The very recent report of a homoacetogenic spirochete as an endosymbiont of a different gut flagellate in another termite species (Ohkuma et al., 2015) suggests that the capacity for reductive acetogenesis may indeed facilitate the colonization of the cytoplasm of termite gut flagellates members of various phyla.

The retention of the biosynthetic pathways for nitrogen fixation and the synthesis of most amino acids and vitamins in the genome of '*Ca.* Adiutrix intracellularis' matches previous reports on other flagellate endosymbionts (Hongoh et al., 2008a, 2008b, Ohkuma et al., 2015). There is general agreement on the hypothesis that such intracellular symbioses have a

nutritional basis (McCutcheon and Moran, 2012). Nitrogen fixation may be the evolutionary driver in the association with bacterial ectosymbionts of gut flagellates in dry-wood termites (Desai and Brune, 2012) – a hypothesis that can possibly be extended to any other associations where the bacteria colonizing the cell surface are exploited as nutrient source via phagocytosis and subsequent digestion (see Brune, 2014). In the case of endosymbionts, however, the exchange of nutrients with the host cell is not a trivial issue. The number of ABC transporters in the genome of '*Ca.* Adiutrix intracellularis' is larger than found, e.g., in the primary endosymbionts of insects (Charles et al., 2015) and includes several homologs putatively involved in the transport of ions or amino acids (Table S4), which may serve to mediate metabolite transfer between symbiont and host.

The capacity for reductive acetogenesis in an endosymbiont is highly unusual and has been found only in the recently discovered '*Candidatus* Treponema intracellularis', whose cells are located close to the hydrogenosomes in the cytoplasm of *Eucomonympha* flagellates in the dampwood termite *Hodotermopsis sjoestedti* (Ohkuma et al., 2015). In view of the extremely high hydrogen partial pressures in the hindgut of *Zootermopsis nevadensis* (Pester and Brune, 2007), it is not clear whether the proximity to the hydrogen source is required to maintain high rates of hydrogen transfer or whether it is merely based on the abundant presence of the organelles in the posterior cell region. Also the reasons for the close situation of '*Ca.* Adiutrix intracellularis' to 'Ca. *Desulfovibrio trichonymphae*' in the anterior cell region and its consequences are open to speculation. Although the metagenome library of the flagellate symbionts did not provide sufficient information to fully reconstruct the metabolism of the 'Ca. *Desulfovibrio trichonymphae*', a provisional analysis of the gene content indicates that this symbiont is a sulfate reducer (Fig. 4) and shows high similarities to the sequences in the genomes of two undescribed *Desulfovibrio* species (strains 3_1_syn3 and 6_1_46AFAA) isolated from the human gut (BioProject accession No.: PRJNA42529 and PRJNA40021, respectively).

The extracellular location of 'Ca. *Desulfovibrio trichonymphae*' on the surface of *T. collaris* may reflect the need for a provision with sulfate via the gut fluid. Interestingly, cells of the related phylotype of '*Ca. Desulfovibrio* trichonymphae' associated with *Trichonympha globulosa* from *Incisitermes marginipennis* are embedded much deeper into invaginations of the cell surface but maintain a connection to the exterior of the host cell (Strassert et al, 2012), whereas cells of '*Ca. Desulfovibrio* trichonymphae' associated with *Trichonympha agilis* from

*Reticulitermes speratus* seem to be true endosymbionts that are completely surrounded by a host membrane (Sato et al., 2009). The consequences of the location for the provision of the symbionts with sulfate are not clear, but the switch to a homoacetogenic metabolism in '*Ca.* Adiutrix intracellularis' may be enforced by a lack of sulfate in its intracellular habitat.

### *Description of* '**Candidatus** *Adiutrix intracellularis*'

'Adiutrix intracellularis' (Ad.iu'trix in'tra.cel.lu.la'ris. L. f. n. *adiutrix*, a female helper or assistant; L. prep. *intra*, within; L. fem. dim. n. *cellula*, a small chamber or cell; L. fem. suff. -*aris*, suffix denoting pertaining to; N.L. fem. adj. *intracellularis*, intracellular; *Adiutrix intracellularis*, an intracellular symbiont.

Properties: Rod-shaped bacteria (approximately 0.5–0.6 in diameter and 0.8–1.9 μm in length) with slightly pointed ends. Form a monophyletic group with the SSU rRNA genes of other *Deltaproteobacteria* from termite guts. Possesses genes encoding for production of acetate from $CO_2$ and $H_2$ (Wood–Ljungdahl pathway) and dinitrogen fixation. Colonize the cytoplasm of the parabasalid flagellate *Trichonympha collaris* in the hindgut of the termite *Zootermopsis nevadensis*.

So far uncultured. The basis of assignment are the SSU rRNA gene sequences of representative phylotypes (Accession No. AB972401; AB894435–AB894480) and hybridization with the specific SSU rRNA-targeted oligonucleotide probe Delta-Tr3-Zn (5'-CTT GAA CCG AAG TTC CTG -3'). A draft genome of strain Adiu1, reconstructed from metagenome sequences, has been deposited in the Integrated Microbial Genomes (IMG) database (IMG Genome ID: 2556793040) and GenBank database (pending).

## Experimental procedures

### *Insects*

Termites were the same as in previous studies (Ikeda-Ohtsubo et al., 2007; Ikeda-Ohtsubo and Brune, 2009; Desai et al., 2010). Colonies were maintained in the laboratory on a diet of pinewood; only pseudergates (workers) were used in the experiments. Cockroaches and *Pachnoda ephippiata* larvae were obtained from commercial breeders (Dietrich et al., 2014).

Insects were dissected and hindgut DNA was extracted as previously described (Ikeda-Ohtsubo et al., 2007).

### *Cloning and sequencing of 16S rRNA genes*

The 16S rRNA genes of uncultured *Deltaproteobacteria* were amplified using the forward primer UncDelta234F [5′-(A/G)GCC(C/T)GCGTGACATTAGAT(T/A)GAT-3′], which was designed to exclusively match all members of the Rs-K70 lineage identified in previous studies, and the general bacteria primer Bact1389R (5′-ACGGGCGGTGTGTACAAG-3′; Osborn et al., 2000). The PCR conditions involved an initial denaturation step of 3 min at 94 °C, 32 cycles of 30 s at 94 °C, 30 s at 66.6 °C, and 45 s at 72 °C, and a final extension step of 7 min at 72 °C. All reactions yielded amplicons of the expected length (~1,150 bp), which were cloned and sequenced as previously described (Ikeda-Ohtsubo et al., 2007). SSU rRNA gene sequences obtained in this study have been deposited at GenBank under accession numbers AB894435–53, AB894461–80, and AB972401.

### *Phylogenetic analysis*

Sequences in this study were imported and aligned against a curated reference database of 16S rRNA genes based on the Silva database (release 119) and including all sequences previously obtained from termites and cockroaches (Mikaelyan et al., 2015). Sequences were analyzed using the tools implemented in the *ARB* software package (Ludwig et al., 2004). Highly variable columns were removed from the alignment using base frequency (< 50% identical bases), and phylogenetic trees were calculated under the maximum-likelihood criterion using *RAxML* with the GTR+Γ+I model and 1,000 bootstrap replicates.

### *FISH analysis*

Fixation of hindgut contents, *in situ* hybridization, washing steps, and epifluorescence microscopy were performed as previously described (Ikeda-Ohtsubo and Brune, 2009). For the specific detection and localization of '*Ca.* Adiutrix intracellularis', we used a newly designed oligonucleotide probe (Delta-ZnvTr3; 5′-CTT GAA CCG AAG TTC CTG-3′) that was specific for all phylotypes of '*Ca.* Adiutrix intracellularis' and a probe (ALF968; Neef et al., 1998) that targeted a wide range of *Proteobacteria* but had one significant mismatch to 16S rRNA of *Desulfovibrio* species. '*Ca.* Desulfovibrio trichonymphae' was localized using a previously published *Desulfovibrio* probe (DSV698; Manz et al., 1998). The probes exactly

matched the SSU rRNA gene sequences of their respective targets and had at least two mismatches to any other clones obtained from the *Trichonympha* suspensions of *Z. nevadensis* (Strassert et al., 2012; this study). *T. collaris* cells were identified with a species-specific probe (ZTcA-Euk; Ikeda-Ohtsubo, 2007). For all probes, formamide was included at concentrations that were optimized for stringent hybridization conditions (20% for probe Delta-ZnvTr3, all others as previously published).

***Electron microscopy***

The contents of two termite hindguts were suspended in Solution U (Trager, 1934). Approximately 120 flagellates identified as *Trichonympha collaris* were collected by micropipetting and fixed in 2.5% glutaraldehyde in 50 mM Soerensen phosphate buffer. Prior to further treatments, the sample was stored overnight at 4 °C. After three rinses in 50 mM cacodylate buffer, the flagellates were post-fixed for 2 h in reduced osmium tetroxide (2% $OsO_4$ plus 3% $K_4[Fe(CN)_6]$, mixed 1:1; Karnovsky, 1971). After three further rinses in 50 mM cacodylate buffer, the flagellates were dehydrated in an increasing series of ethanol and embedded in Spurr's resin (1969). Ultrathin sections were stained with saturated uranyl acetate and lead citrate according to Reynolds (1963) and examined with a Philips EM 208 transmission electron microscope.

***Preparation of symbiont DNA for metagenome sequencing***

Hindgut fluid of ~250 individuals of *Z. nevadensis* was collected in a 2-ml centrifuge tube and gently mixed with 1.2 ml ice-cold Solution U. After about 10 min, the *Trichonympha* cells had sedimented at the bottom of the tube. The supernatant was removed with a micropipette and replaced with fresh solution U. After five such washing steps, the cells were resuspended in isolation buffer (Prechtl et al., 2004) and disrupted using ultrasonication (UP50H, Hielscher, Teltow, Germany; 1-mm tip, 10 cycles of 0.5 s at 30% amplitude).

After removal of flagellate cell debris by centrifugation at 500 × *g* for 2 min, the supernatant was homogenized by pressing it twice through an 18-gauge syringe needle and then filtered through an 80-µm nylon mesh mounted in a Swinex filter holder (Millipore) to remove remaining cell debris and wood particles. The filtrate was treated with DNaseI (RQ1 DNase, Promega) for 15 min to digest flagellate DNA, which dissolved remaining cell aggregates, and subsequently filtered through a 20-µm nylon mesh (Swinex filter holder), and membrane

515 filters of 5-µm and 0.65-µm pore size (Ultrafree-CL centrifugal filter tubes, Amicon). The
516 bacterial cells in the filtrate were sedimented by centrifugation at 8,000 × *g* for 20 min and
517 resuspended in PBS buffer (130 mM NaCl, 7 mM $Na_2HPO_4$ and 3 mM $NaH_2PO_4$, pH 7.4). All
518 procedures were conducted either on ice or at 4 °C.

519 The cell suspension was kept at 65 °C for 10 min to inactivate DNase I, centrifuged again, and
520 resuspended in TE buffer (10 mM Tris-HCl, 1 mM EDTA, pH 8.0). DNA extraction followed
521 a previously described procedure (Herlemann et al., 2009) and yielded 12 µg of high-
522 molecular-weight (>23 kb) DNA.

523 ***Metagenome sequencing and assembly***

524 The DNA of the bacterial symbionts was used to construct both a 16S rRNA gene library and
525 a metagenomic library. The 16S rRNA gene library was constructed and sequenced at the
526 Joint Genome Institute (JGI) following previously described procedures (Warnecke et al.,
527 2007). The resulting sequences were aligned with their closest relatives in our reference
528 database (DictDb; Mikaelyan et al., 2015) and classified into different taxa (Fig. S1). Also the
529 metagenomic DNA was sequenced at the JGI using a combination of Sanger sequencing of a
530 short-insert library and 454-GS20 pyrosequencing following standard procedures. 454
531 sequences were assembled with Newbler then "shredded" into Sanger-like reads that were
532 coassembled with the Sanger data using the Paracel Genome Assembler (pga;
533 www.paracel.com).

534 The original metagenome assembly (GOLD ID: Gp0051377, NCBI BioProject accession:
535 PRJNA78659) consisted of 24.9 Mbp of metagenome data in 22,673 scaffolds. Scaffolds with
536 a length of more than 1,000 bp (11.9 Mb, 4,237 scaffolds) were classified using PhyloPythiaS
537 (Patil et al., 2012; Gregor et al. 2014), which yielded 13 phylogenetic groups (Table S1). The
538 training data included generic models representing all clades of bacteria and sample-specific
539 generic models for the major bacterial symbionts identified in the 16S rRNA gene library
540 obtained from the same DNA preparation (Table S1). As specific training data for '*Ca.*
541 Adiutrix intracellularis', we selected several large scaffolds (~100 kb in total) that contained
542 either the SSU rRNA gene of Adiu1 or single-copy phylogenetic marker genes of
543 *Deltaproteobacteria* other than *Desulfovibrionaceae*.

544 In addition to the 144 scaffolds assigned to '*Ca.* Adiutrix intracellularis', we identified 11
545 scaffolds using a combination of the following criteria: (i) the average G+C content was

closer to that of *bona fide* Adiu1 sequences (43.3 %) than to sequences of '*D. trichonymphae*'(55 %), (ii) the coding sequences (CDS) in the scaffold had the highest similarity to genes of *Deltaproteobacteria* species in the GenBank database and were more similar to *Desulfobacterium*, *Syntrophobacter*, or *Desulfobacca* spp. than to *Desulfovibrio* spp., and (iii) the scaffolds did not contain CDS with a high similarity to other bacterial lineage represented in the 16S rRNA gene library (Table S1). Scaffolds matching these criteria were further validated by verifying the phylogenetic position of least one CDS in the scaffold using BLASTP (http://blast.ncbi.nlm.nih.gov).

The resulting draft genome of strain Adiu1 was uploaded to the Integrated Microbial Genomes Expert Review (IMG-ER) platform (Markowitz et al, 2009), where gene-calling and automatic functional annotation were performed. Metabolic reconstruction of Adiu1 was performed based on a list of functional genes involved in important metabolic pathways (Table S2), each of which were automatically and then manually curated by comparing the predicted protein sequences with those in GenBank and IMG databases. The final annotation of the draft genome of '*Ca.* Adiutrix intracellularis' strain Adiu1 (IMG Genome ID: 2556793040) has been submitted to Genbank (pending).

## Acknowledgments

This work was financed in part by a grant of the Deutsche Forschungsgemeinschaft (DFG) in the Collaborative Research Center Transregio 1 (SFB-TR1) and by the Max Planck Society. Other parts of this work were funded by the Community Sequencing Program of the U.S. Department of Energy Joint Genome Institute, a DOE Office of Science User Facility whose work is supported by the Office of Science of the U.S. Department of Energy under Contract No. DE-AC02-05CH11231. W.I.-O. was supported by stipends of the International Max Planck Research School for Molecular, Cellular, and Environmental Microbiology (IMPRS-Mic) and the Deutscher Akademischer Austauschdienst (DAAD).

We thank the members of the JGI production sequencing, quality assurance, and genome biology programs and the IMG team for their assistance in genome sequencing, assembly, annotation, and loading of the genome into IMG.

## References


Bouma, C.L., and Roseman, S. (1996) Sugar transport by the marine chitinolytic bacterium *Vibrio furnissii*. Molecular cloning and analysis of the mannose/glucose permease. *J Biol Chem* **271:** 33468–33475.

Breznak, J.A. (2000) Ecology of prokaryotic microbes in the guts of wood- and litter-feeding termites. In *Termites: Evolution, Sociality, Symbiosis, Ecology*. Abe, T., Bignell, D. E. and Higashi, M. (eds). Dordrecht: Kluwer, pp. 209–231.

Breznak, J.A., and Leadbetter, J.R. (2006) Termite gut spirochetes. In *The Prokaryotes, 3rd edn., Vol. 7*. Dworkin, M., Falkow, S., Rosenberg, E., Schleifer, K-H., and Stackebrandt, E. (eds). New York, NY, USA: Springer, pp. 318–329.

Brugerolle, G., and Radek, R. (2006) Symbiotic protozoa of termites. In *Intestinal Microorganisms of Termites and Other Invertebrates*. König, H., and Varma, A. (eds). Berlin: Springer, pp. 243–269.Brune, A. (2014) Symbiotic digestion of lignocellulose in termite guts. *Nat Rev Microbiol* **12:** 168–180.

Brune, A., and Ohkuma, M. (2011) Role of the termite gut microbiota in symbiotic digestion. In *Biology of Termites: A Modern Synthesis*. Bignell, D.E., Roisin, Y., and Lo, N. (eds). Dordrecht: Springer, pp. 439–475.

Charles, H., Balmand, S., Lamelas, A., Cottret, L., Pérez-Brocal, V., Burdin, B., et al. (2015) A genomic reappraisal of symbiotic function in the aphid/*Buchnera* symbiosis: reduced transporter sets and variable membrane organisations. *PLoS One* **6:** e29096.

Cleveland, L.R. (1925) The ability of termites to live perhaps indefinitely on a diet of pure cellulose. *Biol Bull* **48:** 289–293.

596 Carpenter, K.J., Chow, L., and Keeling, P.J. (2009) Morphology, phylogeny, and diversity of
597 *Trichonympha* (Parabasalia: Hypermastigida) of the wood-feeding cockroach
598 *Cryptocercus punctulatus*. J Eukaryot Microbiol **56:** 305–313.

599 Desai, M.S., Strassert, J.F.H., Meuser, K., Hertel, H., Ikeda-Ohtsubo, W., Radek, R., and
600 Brune, A. (2010) Strict cospeciation of devescovinid flagellates and *Bacteroidales*
601 ectosymbionts in the gut of dry-wood termites (*Kalotermitidae*). *Environ Microbiol* **12:**
602 2120–2132.

603 Desai, M.S., and Brune, A. (2012) *Bacteroidales* ectosymbionts of gut flagellates shape the
604 nitrogen-fixing community in dry-wood termites. *ISME J* **6**: 1302–1313.

605 Dietrich, C., Köhler, T., and Brune, A. (2014) The cockroach origin of the termite gut
606 microbiota: patterns in bacterial community structure reflect major evolutionary events.
607 *Appl Environ Microbiol* **80:** 2261–2269.

608 Fröhlich, J., Sass, H., Babenzien, H.-D., Kuhnigk, T., Varma, A., Saxena, S., et al. (1999)
609 Isolation of *Desulfovibrio intestinalis* sp. nov., from the hindgut of the lower termite
610 *Mastotermes darwiniensis*. *Can J Microbiol* **45**: 145–152.

611 Garcia Martin, H., Ivanova, N., Kunin, V., Warnecke, F., Barry, K.W., et al. (2006)
612 Metagenomic analysis of two enhanced biological phosphorus removal (EBPR) sludge
613 communities. *Nat Biotechnol* **24:** 1263–1269.

614 Graber, J.R., and Breznak, J.A. (2004) Physiology and nutrition of *Treponema primitia*, an
615 $H_2$/$CO_2$-acetogenic spirochete from termite hindguts. *Appl Environ Microbiol* **70:** 1307–
616 1314.

617 Graber, J.R., and Breznak, J.A. (2005) Folate cross-feeding supports symbiotic
618 homoacetogenic spirochetes. *Appl Environ Microbiol* **71:** 1883–1889.

619 Gregor, I., Dröge, J., Schirmer, M., Quince, C., and McHardy, A.C. (2014) PhyloPythiaS+: A
620 self training method for the rapid reconstruction of low-ranking taxonomic bins from
621 metagenomes. *ArXiv e-prints* 1–48.

622 Herlemann, D.P.R., Geissinger, O., Ikeda-Ohtsubo, W., Kunin, V., Sun, H., Lapidus, A.,
623 Hugenholtz, P., and Brune, A. (2009) Genomic analysis of "*Elusimicrobium minutum*,"
624 the first cultivated representative of the phylum "*Elusimicrobia*" (formerly Termite Group
625 1). *Appl Environ Microbiol* **75**: 2841–2849.

626 Hongoh, Y., and Ohkuma, M. (2010) Termite gut flagellates and their methanogenic and
627 eubacterial symbionts. In *(Endo)symbiotic Methanogenic Archaea*. Hackstein, J.H.P. (ed).
628 Heidelberg: Springer, pp. 55–79.

629 Hongoh, Y., Ohkuma, M., and Kudo, T. (2003). Molecular analysis of bacterial microbiota in
630 the gut of the termite *Reticulitermes speratu*s (Isoptera, Rhinotermitidae). *FEMS*
631 *Microbiol Ecol* **44**: 231–242.

632 Hongoh, Y., Deevong, P., Inoue, T., Moriya, S., Trakulnaleamsai, S., Ohkuma, M.,
633 Vongkaluang, C., Noparatnaraporn, N., and Kudo, T. (2005) Intra- and interspecific
634 comparisons of bacterial diversity and community structure support coevolution of gut
635 microbiota and termite host. *Appl Environ Microbiol* **71**: 6590–6599.

636 Hongoh, Y., Sharma, V.K., Prakash, T., Noda, S., Toh, H., Taylor, T.D., et al. (2008a) Genome
637 of an endosymbiont coupling $N_2$ fixation to cellulolysis within protist cells in termite gut.
638 *Science* **322**: 1108–1109.

639 Hongoh, Y., Sharma, V.K., Prakash, T., Noda, S., Taylor, T.D., Kudo, T., et al. (2008b)
640 Complete genome of the uncultured Termite Group 1 bacteria in a single host protist cell.
641 *Proc Natl Acad Sci USA* 105: 5555–5560.

642 Hungate, R.E. (1943) Quantitative analysis on the cellulose fermentation by termite protozoa.
643 *Ann Entomol Soc Am* **36:** 730–739.

644 Ikeda-Ohtsubo, W. (2007) *Endomicrobia* in termite guts: symbionts within a symbiont.
645 Phylogeny, cospeciation with host flagellates, and preliminary genome analysis.
646 Dissertation, Philipps-Universität Marburg, Germany.

647 Ikeda-Ohtsubo, W., and Brune, A. (2009) Cospeciation of termite gut flagellates and their
648 bacterial endosymbionts: *Trichonympha* species and '*Candidatus* Endomicrobium
649 trichonymphae'. *Mol Ecol* **18**: 332–342.

650 Ikeda-Ohtsubo, W., Desai, M., Stingl, U., and Brune. A. (2007) Phylogenetic diversity of
651 "*Endomicrobia*" and their specific affiliation with termite gut flagellates. *Microbiology*
652 **153:** 3458–3465.

653 Ikeda-Ohtsubo, W., Faivre, N., and Brune, A. (2010) Putatively free-living "Endomicrobia" –
654 ancestors of the intracellular symbionts of termite gut flagellates? *Environ Microbiol Rep*
655 **2**: 554–559.

656 Javelle, A., Serveri, E., Thornton, J., and Merrick, M. (2004) Ammonium sensing in
657 *Escherichia coli*: role of the ammonium transporter AmtB and AmtB-GlnK complex
658 formation. *J Biol Chem* **279:** 8530–8538.

659 Karnovsky, M.J. (1971) Use of ferrocyanide-reduced osmium tetroxide in electron
660 microscopy. Abstract 284. In *Proceedings of the 11th Annual Meeting of the American*
661 *Society for Cell Biology*. New Orleans, p. 146.

662 Kim, M., Le, H., McInerney, M.J., and Buckel, W. (2013) Identification and characterization
663 of *Re*-citrate synthase in *Syntrophus aciditrophicus*. *J Bacteriol* **195:** 1689–1696.

664 Kirby, H. Jr (1932) Flagellates of the genus *Trichonympha* in termites. *Univ Calif Publ Zool*,
665 **37**: 349–476.

666 Köhler, T., Dietrich, C., Scheffrahn, R.H., and Brune, A. (2012) High-resolution analysis of
667 gut environment and bacterial microbiota reveals functional compartmentation of the gut
668 in wood-feeding higher termites (*Nasutitermes* spp.). *Appl Environ Microbiol* **78**: 4691–
669 4701.

670 Kuever, J. (2014) The Family Desulfobacteraceae. In *The Prokaryotes, Vol. 10:*
671 *Deltaproteobacteria* and *Epsilonproteobacteria*. Berlin: Springer, pp. 45–73.

672 Kuhnigk, T., Branke, J., Krekeler, D., Cypionka, H., and König, H. (1996) A feasible role of
673 sulfate-reducing bacteria in the termite gut. *Syst Appl Microbiol* **19**: 139–149.

674 Lang, K., Schuldes, J., Klingl, A., Poehlein, A., Daniel, R., and Brune, A. (2015) New mode
675 of energy metabolism in the seventh order of methanogens as indicated by comparative
676 genome analysis of "*Candidatus* Methanoplasma termitum". *Appl Environ Microbiol* **81:**
677 1338–1352.

678 Leadbetter, J. R., Schmidt, T. M., Graber, J. R., and Breznak, J. A. (1999) Acetogenesis from
679 $H_2$ plus $CO_2$ by spirochetes from termite guts. *Science* **283:** 686–689.

680 Lee, M. J., Schreurs, P. J., Messer, A.C., and Zinder, S.H. (1987) Association of methanogenic
681 bacteria with flagellated protozoa from a termite hindgut. *Curr Microbiol* **15**: 337–341.

682 Leidy, J. (1881) The parasites of the termites. *J Acad Nat Sci Philadelphia 2nd Ser* **8**: 425–
683 447.

684 Ljungdahl, L.G. (1994) The acetyl-CoA pathway and the chemiosmotic generation of ATP
685 during acetogenesis. In *Acetogenesis*. Ferry, J.G. (eds). New York, NY, USA: Chapman
686 & Hall, pp. 63–87.

687 Ludwig, W., Strunk, O., Westram, R., Richter, L., Meier, H., Yadhukumar, et al. (2004) ARB:
688 a software environment for sequence data. *Nucleic Acids Res* **32**: 1363–1371.

689 Manz, W., Eisenbrecher, M., Neu, T.R., and Szewzyk, U. (1998) Abundance and spatial
690 organization of Gram-negative sulfate-reducing bacteria in activated sludge investigated
691 by in situ probing with specific 16S rRNA targeted oligonucleotides. *FEMS Microbiol*
692 *Ecol* **25**: 43–61.

693 Markowitz, V.M., Ivanova, N.N., Chen, I.M., Chu, K., and Kyrpides, N.C. (2009) IMG ER: a
694 system for microbial genome annotation expert review and curation. *Bioinformatics* **25**:
695 2271–2278.

696 Malki, S., Saimmaine, I., De Luca, G., Rousset, M., Dermoun, Z. and Belaich, J.P. (1995)
697 Characterization of an operon encoding an NADP-reducing hydrogenase in *Desulfovibrio*
698 *fructosovorans*. *J Bacteriol* **177:** 2628–2636.

699 Matson, E.G., Zhang, X., and Leadbetter, J.R. (2010) Selenium controls transcription of
700 paralogous formate dehydrogenase genes in the termite gut acetogen, *Treponema*
701 *primitia*. *Environ Microbiol* **12**: 2245–2258.

702 McCutcheon, J.P., and Moran, N.A. (2012) Extreme genome reduction in symbiotic bacteria.
703 *Nat Rev Microbiol* **10:** 13–26.

704 Messer, A.C., and Lee, M.J. (1989) Effect of chemical treatments on methane emission by the
705 hindgut microbiota in the termite *Zootermopsis angusticollis*. *Microb Ecol* **18**: 275–284.

706 Mikaelyan, A., Köhler, T., Lampert, N., Rohland, J., Boga, H., Meuser, K., and Brune, A.
707 (2015) Classifying the bacterial gut microbiota of termites and cockroaches: a curated
708 phylogenetic reference database (DictDb). Syst Appl Microbiol,
709 http://dx.doi.org/10.1016/j.syapm.2015.07.004.

710 Mock, J., Wang, S., Huang, H., Kahnt, J., and Thauer, R.K. (2014) Evidence for a
711 hexaheteromeric methylenetetrahydrofolate reductase in *Moorella thermoacetica*. *J*
712 *Bacteriol* **196:** 3303–3314

713 Moparthi, V.K., and Hägerhäll, C. (2011) The evolution of respiratory chain complex I from a
714 smaller last common ancestor consisting of 11 protein subunits. *J Mol Evol* **72:** 484–497
715 Moran, N.A., McCutcheon, J.P., and Nakabachi, A. (2008). Genomics and evolution of
716 heritable bacterial symbionts. *Ann Rev Genetics* **42**: 165–190.
717 Neef, A., Amann, R., Schlesner, H., and Schleifer, K.-H. (1998) Monitoring a widespread
718 bacterial group: in situ detection of planctomycetes with 16S rRNA-targeted probes.
719 *Microbiology* **144**: 3257–3266.
720 Noda, S., Ohkuma, M., Usami, R., Horikoshi, K., and Kudo, T. (1999) Culture-independent
721 characterization of a gene responsible for nitrogen fixation in the symbiotic microbial
722 community in the gut of the termite *Neotermes koshunensis*. *Appl Environ Microbiol* **65:**
723 4935–4942.
724 Noda, S., Hongoh, Y., Sato, T., and Ohkuma, M. (2009) Complex coevolutionary history of
725 symbiotic Bacteroidales bacteria of various protists in the gut of termites. *BMC Evol Biol*
726 **9:** 158.
727 Ohkuma, M., and Brune, A. (2011) Diversity, structure, and evolution of the termite gut
728 microbial community. In *Biology of Termites: A Modern Synthesis*. Bignell, D.E., Roisin,
729 Y., Lo, N. (eds). Dordrecht: Springer, pp. 413–438.
730 Ohkuma, M., Iida, T., Ohtoko, K., Yuzawa, H., Noda, S., Viscogliosi, E., and Kudo, T. (2005)
731 Molecular phylogeny of parabasalids inferred from small subunit rRNA sequences, with
732 emphasis on the *Hypermastigea*. *Mol Phylogenet Evol* **35**: 646–655.
733 Ohkuma, M., Noda, S., Hongoh, Y., Nalepa, C.A., Inoue, T. (2009) Inheritance and
734 diversification of symbiotic trichonymphid flagellates from a common ancestor of
735 termites and the cockroach *Cryptocercus*. Proc R Soc B **276:** 239–245.

Ohkuma, M., Noda, S., Hattori, S., Iida, T., Yuki, M., Starns, D., Inoue, J.-I., Darby, A.C., Hongoh, Y. (2015) Acetogenesis from $H_2$ plus $CO_2$ and nitrogen fixation by an endosymbiotic spirochete of a termite-gut cellulolytic protist. *Proc Natl Acad Sci USA*, http://dx.doi.org/10.1073/pnas.1423979112

Osborn, A.M., Moore, E.R., and Timmis, K.N. (2000) An evaluation of terminal-restriction fragment length polymorphism (T-RFLP) analysis for the study of microbial community structure and dynamics. *Environ Microbiol* **2:** 39–50.

Ottesen, E.A., Hong, J.W., Quake, S.R., and Leadbetter, J. R. (2006). Microfluidic digital PCR enables multigene analysis of individual environmental bacteria. *Science* **314**: 1464–1467.

Patil, K.R., Roune, L., and McHardy, A.C. (2012) The PhyloPythiaS web server for taxonomic assignment of metagenome sequences. *PLoS ONE* **7**: e38581

Pester, M., and Brune, A. (2006) Expression profiles of fhs (FTHFS) genes support the hypothesis that spirochaetes dominate reductive acetogenesis in the hindgut of lower termites. *Environ Microbiol* **8:** 1261–1270.

Pester, M., and Brune, A. (2007) Hydrogen is the central free intermediate during lignocellulose degradation by termite gut symbionts. *ISME J* **1:** 551–565.

Poehlein, A., Daniel, R., Schink, B., and Simeonova, D.D. (2013) Life based on phosphite: a genome-guided analysis of *Desulfotignum phosphitoxidans*. *BMC Genomics* **14**: 753.

Prechtl, J., Kneip, C., Lockhart, P., Wenderoth, K., and Maier, U.-G. (2004) Intracellular spheroid bodies of *Rhopalodia gibba* have nitrogen-fixing apparatus of cyanobacterial origin. *Mol Biol Evol* **21**: 1477–81.

758 Rodionov, D.A., Dubchak, I., Arkin, A., Alm, E., and Gelfand, M.S. (2004) Reconstruction of
759 regulatory and metabolic pathways in metal-reducing δ-proteobacteria. *Genome Biol* **5**:
760 R90.

761 Reynolds, E.S. (1963) The use of lead citrate at high pH as an electron-opaque stain in
762 electron microscopy. *J Cell Biol* **17**: 208–212.

763 Rosenthal, A.Z., Zhang, X., Lucey, K.S., Ottesen, E.A., Trivedi, V., Choi, H.M.T., Pierce,
764 N.A., and Leadbetter, J.R. (2013) Localizing transcripts to single cells suggests an
765 important role of uncultured deltaproteobacteria in the termite gut hydrogen economy.
766 *Proc Natl Acad Sci USA* **110:** 16163–16168.

767 Sato, T., Hongoh, Y., Noda, S., Hattori, S., Ui, S., and Ohkuma, M. (2009) *Candidatus*
768 Desulfovibrio trichonymphae, a novel intracellular symbiont of the flagellate
769 *Trichonympha agilis* in termite gut. *Environ Microbiol* **11**: 1007–1015.

770 Schink, B., Thiemann, V., Laue, H., and Friedrich, M.W. (2002) *Desulfotignum*
771 *phosphitoxidans* sp. nov., a new marine sulfate reducer that oxidizes phosphite to
772 phosphate. *Arch Microbiol* **177**: 381–391.

773 Schuchmann, K., and Müller, V. (2012) A bacterial electron-bifurcating hydrogenase. *J Biol*
774 *Chem* **287:** 31165–3117.

775 Schuchmann, K., and Müller, V. (2014) Autotrophy at the thermodynamic limit of life: a
776 model for energy conservation in acetogenic bacteria. *Nat Rev Microbiol* **12:**809–821.

777 Schnell, S., Bak, F., and Pfennig, N. (1989) Anaerobic degradation of aniline and
778 dihydroxybenzenes by newly isolated sulfate-reducing bacteria and description of
779 *Desulfobacterium anilini*. *Arch Microbiol* **152;** 556–563.

780 Shinzato, N., Muramatsu, M., Matsui, T., and Watanabe,Y. (2007) Phylogenetic analysis of the
781 gut bacterial microflora of the fungus-growing termite *Odontotermes formosanus*. *Biosci*
782 *Biotechnol Biochem* **71:** 906–915.

783 Spurr, A.R. (1969) A low-viscosity epoxy resin embedding medium for electron microscopy. *J*
784 *Ultrastruct Res* **26**: 31–43.

785 Stingl, U., Radek, R., Yang, H., and Brune, A. (2005) '*Endomicrobia*': cytoplasmic symbionts
786 of termite gut protozoa form a separate phylum of prokaryotes. *Appl Environ Micobiol*
787 **71:** 1473–1479.

788 Suzuki, D., Li, Z., Cui, X., Zhang, C., and Katayama, A. (2014) Reclassification of
789 *Desulfobacterium anilini* as *Desulfatiglans anilini* comb. nov. within *Desulfatiglans* gen.
790 nov., and description of a 4-chlorophenol-degrading sulfate-reducing bacterium,
791 *Desulfatiglans parachlorophenolica* sp. nov. *Int J Syst Evol Microbiol* **64:** 3081–3086.

792 Strassert, J.F.H., Köhler, T., Wienemann, T.H.G., Ikeda-Ohtsubo, W., Faivre, N.,
793 Franckenberg, S., Plarre, R., Radek, R., and Brune, A. (2012) '*Candidatus* Ancillula
794 trichonymphae', a novel lineage of endosymbiotic *Actinobacteria* in termite gut
795 flagellates of the genus *Trichonympha*. *Environ Microbiol* **14**: 3259–3270.

796 Tai, V., and Keeling, P.J. (2013) Termite hindguts and the ecology of microbial communities
797 in the sequencing age. *J Euk Microbiol*, **60**: 421–428.

798 Trager, W. (1934) The cultivation of a cellulose-digesting flagellate, *Trichomonas*
799 *termopsidis*, and of certain other termite protozoa. *Biol Bull* **66**: 182–190.

800 Trinkerl, M., Breunig, A., Schauder, R. and König, H. (1990) *Desulfovibrio termitidis* sp.
801 nov., a carbohydrate-degrading sulfate-reducing bacterium form the hindgut of a termite.
802 *Syst Appl Microbiol* **13**: 372–377

803 Wang, S., Huang, H., Kahnt, J., and Thauer, R.K. (2013) A reversible electron-bifurcating
804 ferredoxin- and NAD dependent [FeFe]-hydrogenase (HydABC) in *Moorella*
805 *thermoacetica*. *J Bacteriol* **195:** 1267–1275.

806 Warnecke, F., Luginbühl, P., Ivanova, N., Ghassemian, M., Richardson, T.H., Stege, J.T., et al.
807 (2007) Metagenomic and functional analysis of hindgut microbiota of a wood feeding
808 higher termite. *Nature* **450**: 560–565.

809 Welte, C., and Deppenmeier, U. (2014) Bioenergetics and anaerobic respiratory chains of
810 aceticlastic methanogens. *Biochim Biophys Acta* **1837:** 1130–1147.

811 Widdel, F., and Bak, F. (1992) Gram-negative mesophilic sulfate-reducing bacteria. In *The*
812 *Prokaryotes, 2nd edn, Vol. 4* (Balows A., Trüper H.G., Dworkin M., Harder W., Schleifer
813 K.-H. (Eds). New York, NY, USA: Springer, pp. 3352–3378.

814 Yang, J., Xie, X., Wang, X., Dixon, R., and Wang, Y.P. (2014) Reconstruction and minimal
815 gene requirements for the alternative iron-only nitrogenase in *Escherichia coli*. *Proc Natl*
816 *Acad Sci USA* **111**: 3718–3725.

817 Zhang, X., Matson, E.G., and Leadbetter, J.R. (2011) Genes for selenium dependent and
818 independent formate dehydrogenase in the gut microbial communities of three lower,
819 wood-feeding termites and a wood-feeding roach. *Environ Microbiol* **13**: 307–323.

820 Zinoni, F., Birkmann, A., Leinfelder, W., and Böck, A. (1987) Cotranslational insertion of
821 selenocysteine into formate dehydrogenase from *Escherichia coli* directed by a UGA
822 codon. *Proc Natl Acad Sci USA* **84:** 3156–3160.

## Figure legends

**Fig. 1.** Phylogenetic tree illustrating the position of '*Candidatus* Adiutrix intracellularis' within the Rs-K70 group and relative to other *Deltaproteobacteria*. The maximum-likelihood tree is based on an unambiguous alignment of 16S rRNA gene sequences (1,271 nucleotide positions) and includes all phylotypes of the intestinal cluster obtained in this and previous studies (for more details of the Rs-K70 group, see Fig. S1). Highly supported nodes (1,000 bootstraps) are marked (○, > 70%; ●, > 95%). The tree was rooted using representatives from the other classes of *Proteobacteria* (not shown). Bar = 0.1 substitutions per site.

**Fig. 2.** Photomicrographs of *Trichonympha* flagellates and associated bacterial symbionts from the hindgut of *Zootermopsis nevadensis*.

A. Epifluorescence image of a *Trichonympha* suspension simultaneously hybridized with a fluorescein-labelled universal bacteria probe (EUB338, green) and a Cy3-labelled probe specific for '*Ca.* Adiutrix intracellularis' (Delta-ZnvTr3; appears yellow in the overlay). Bar = 100 µm.

B. Phase-contrast image of a *Trichonympha collaris* cell, showing the nucleus and wood particles in the posterior region. The arrow marks the outer cytoplasm of the anterior region, which consists of cytoplasmic protrusions between the flagella. Bar = 50 µm.

C. Epifluorescence image of a *T. collaris* cell hybridized with probe Delta-ZnvTr3, showing the distribution of '*Ca.* Adiutrix intracellularis' across the entire host cell. Bar = 50 µm.

D. The anterior pole of a *T. collaris* cell simultaneously hybridized with the same probe (Delta-ZnvTr3; red) and a fluorescein-labelled probe (DSV698, green) matching the *Desulfovibrio* symbiont; autofluorescent wood particles in vacuoles appear yellow. Bar = a, 100 µm; b–c, 50 µm; d, 10 µm.

**Fig. 3.** Transmission electron micrographs of *Trichonympha collaris* and its associated symbionts.

A. Ultrathin section of the posterior part of the host cell, showing endosymbiotic '*Ca.* Adiutrix intracellularis' (arrows) surrounded by hydrogenosomes (h); the inset shows a longitudinal section of the endosymbiont. Bar = 1 µm (inset: 0.2 µm).

B. Radial section of the cytoplasmic lamellae between the flagella (fl) in the collar region, showing endosymbiotic '*Ca.* Adiutrix intracellularis' (black arrows) and ectosymbiotic '*Ca.* Desulfovibrio trichonymphae' (white arrows). Bar = 1 µm.
C. Longitudinal section of the same region, showing '*Ca.* Adiutrix intracellularis' (black arrows) and '*Ca.* Desulfovibrio trichonymphae' (white arrows) and multiple rows of flagella (fl). Bar = 1 µm.

**Fig. 4.** Wood-Ljungdahl pathway for reductive acetogenesis and energy conservation in '*Ca.* Aduitrix intracellularis'. The scheme is based on the annotation of the draft genome of strain Adiu1 (Table S4). Colors indicate the phylogenetic context of the respective homologs in published genomes: blue, *Deltaproteobacteria* (sulfate reducers); red, *Clostridiales* (homoacetogens); green, *Treponema primitia* (homoacetogen). A detailed analysis of each gene homolog potentially involved in the Wood-Ljungdahl pathway and the energy metabolism in this context is shown in Table S5. The hypothetical link (dotted lines) between the energy-converting 11-subunit complex and methylene-THF reductase is discussed in the text.

**Fig. 5.** Metabolic map of '*Ca.* Aduitrix intracellularis' reconstructed from the draft genome of strain Adiu1. Important cofactors in energy metabolism (in red) and the links to the pathways of amino acid biosynthesis (in blue) and vitamin and cofactor biosynthesis (in orange) are emphasized. Abbreviations: THF, tetrahydrofolate; HCO-THF, 10-formyl-tetrahydrofolate; $CH_2$=THF, 5,10-methylenetetrahydrofolate; $CH_3$-THF, 5-methyltetrahydrofolate, CFeSP, corrinoid iron–sulfur protein; Acetyl-P; acetyl phosphate; G1P, glucose 1-phosphate; G6P, glucose 6-phosphate; M6P, mannose 6-phosphate; F6P, fructose 6-phosphate; FBP, fructose 1,6-bisphosphate; GAP, glyceraldehyde 3-phosphate; BPG, 1,3-bisphosphoglycerate; 3PG, 3-phosphoglycerate, 2PG, 2-phosphoglycerate; PEP, phosphoenolpyruvate; E4P, erythrose 4-phosphate; S7P, sedoheptulose 7-phosphate; X5P, xylulose 5-phosphate; R5P, ribose-5-phosphate; Ru5P, ribulose 5-phosphate; PRPP, phosphoribosyl pyrophosphate; Ala, alanine; Arg, arginine; Asp, aspartate; Asn, asparagine; Glu, glutamate; Gln, glutamine; Gly, glycine; Ile, isoleucine; Leu, leucine; Lys, lysine; Phe, phenylalanine; Pro, proline; Ser, serine; Thr, threonine; Trp, tryptophan; Tyr, tyrosine; Val, valine.

Fig. 1

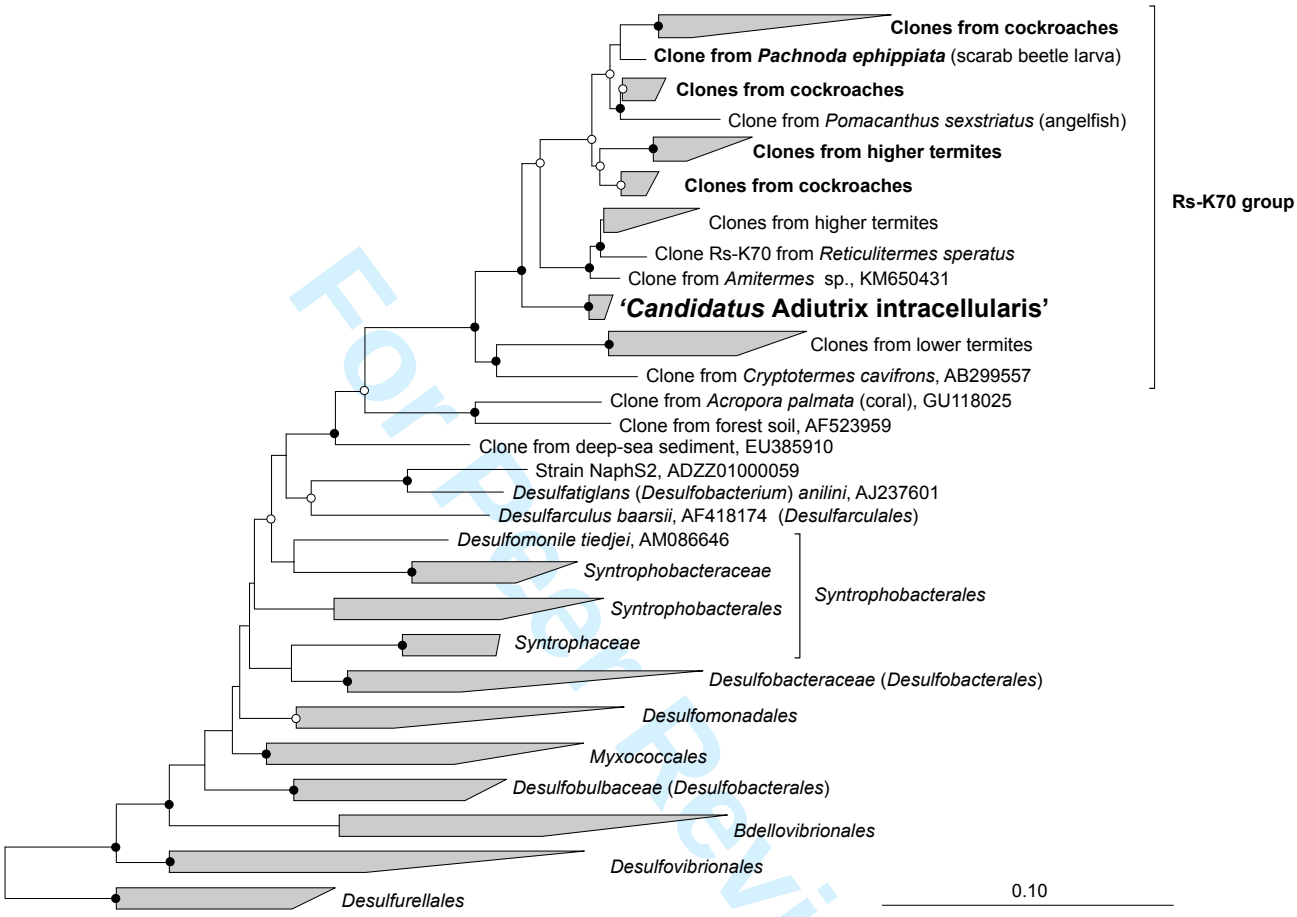

Fig. 2

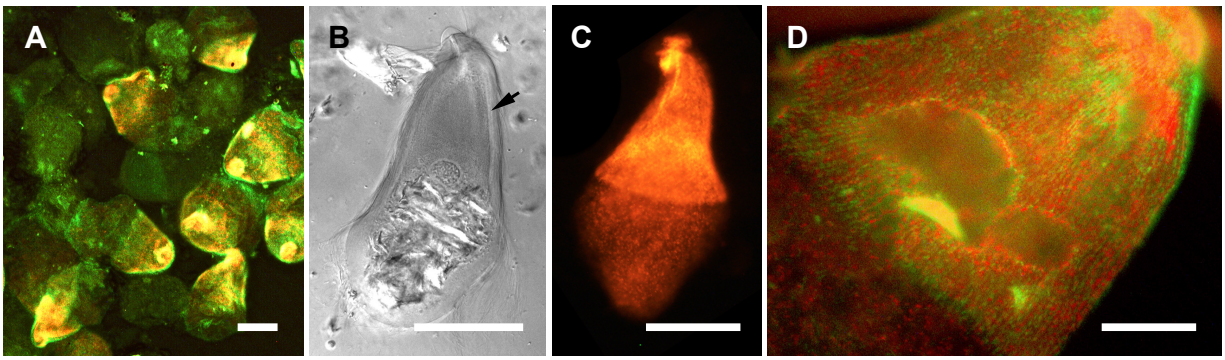

Fig. 3

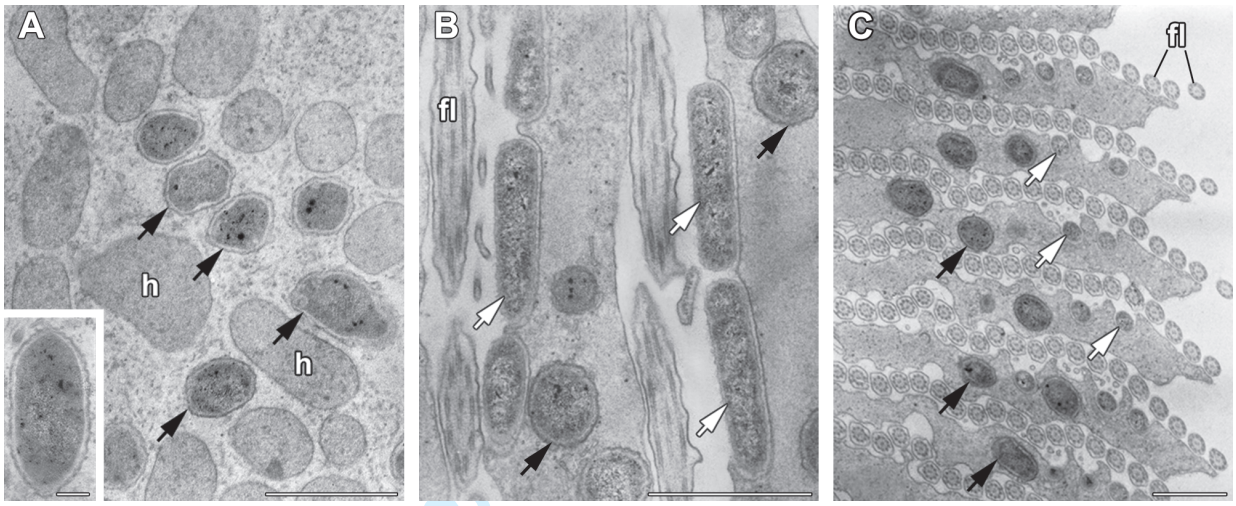

Fig. 4

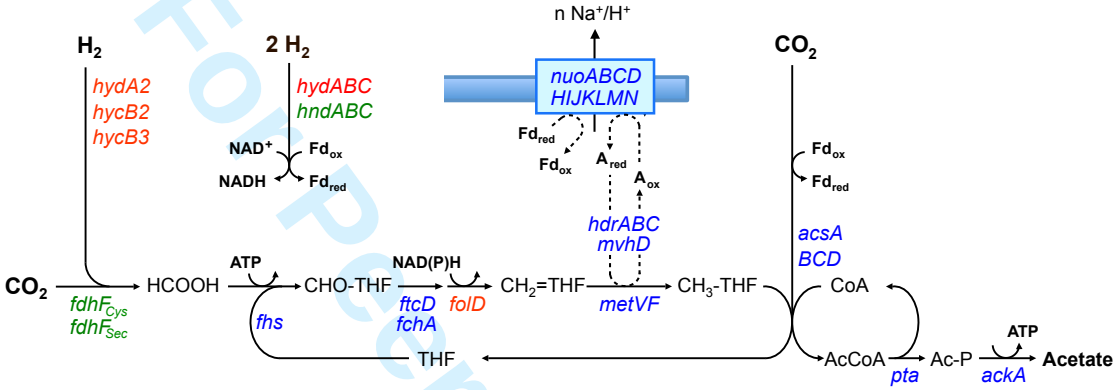

Fig. 5